

Controllable Fusion of Human Brain Organoids Using Acoustofluidics

Zheng Ao,¹ Hongwei Cai,¹ Zhu hao Wu,¹ Jonathan Ott,¹ Huiliang Wang,²
Ken Mackie,³ and Feng Guo,^{1*}

1. Department of Intelligent Systems Engineering, Indiana University, Bloomington, IN 47405, United States
2. Department of Biomedical Engineering, The University of Texas at Austin, TX, 78712, United States
3. Gill Center for Biomolecular Science, and Department of Psychological and Brain Sciences, Indiana University, Bloomington, IN 47405, United States

*Corresponding email: fengguo@iu.edu

Supplementary Figures

- **Figure S1. Fabrication and characterization of human forebrain organoids (hFOs).**
- **Figure S2. Fabrication and characterization of human midbrain organoids (hMOs).**
- **Figure S3. Gene expression analysis of hFOs and hMOs.**
- **Figure S4. Device image and numerical simulation.**
- **Figure S5. Viability test of organoids after the controllable fusion.**
- **Figure S6. Definition of *toward* and *away* assembloid.**
- **Figure S7. Confirmation of TH neuron origin in the assembloid.**

Supplementary Tables

- **Table S1 Reagents and resources**
- **Table S2 Medium composition for human forebrain organoid fabrication**
- **Table S3 Medium composition for human midbrain organoid fabrication**
- **Table S4 Comparison of current spheroid/organoid assembly methods**

Supplementary Movies

- **Movie S1. Simulation of rotational manipulation**
- **Movie S2. Simulation of transportation via phase shift**
- **Movie S3. Acoustofluidic rotation of an hFO**
- **Movie S4. The directional fusion of an hFO and an hMO**
- **Movie S5. Spontaneous firing of hMO-hFO assembloids**

Supplementary Figures

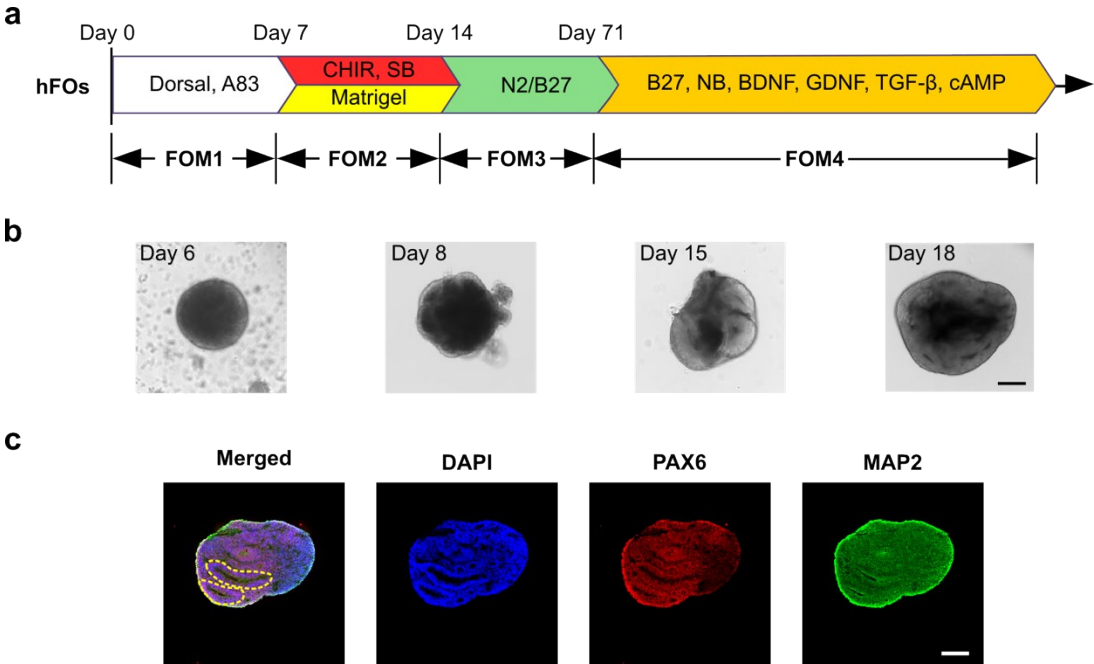


Figure S1. Fabrication and characterization of human forebrain organoids (hFOs). (a) Schematics showing human forebrain organoid fabrication protocol. (b) Human forebrain organoid maturation before the assembly process. (c) Immunofluorescence staining showing human forebrain organoid formation with PAX6+ neural progenitor cells and MAP2+ mature neurons. Scale bar: 200 μ m

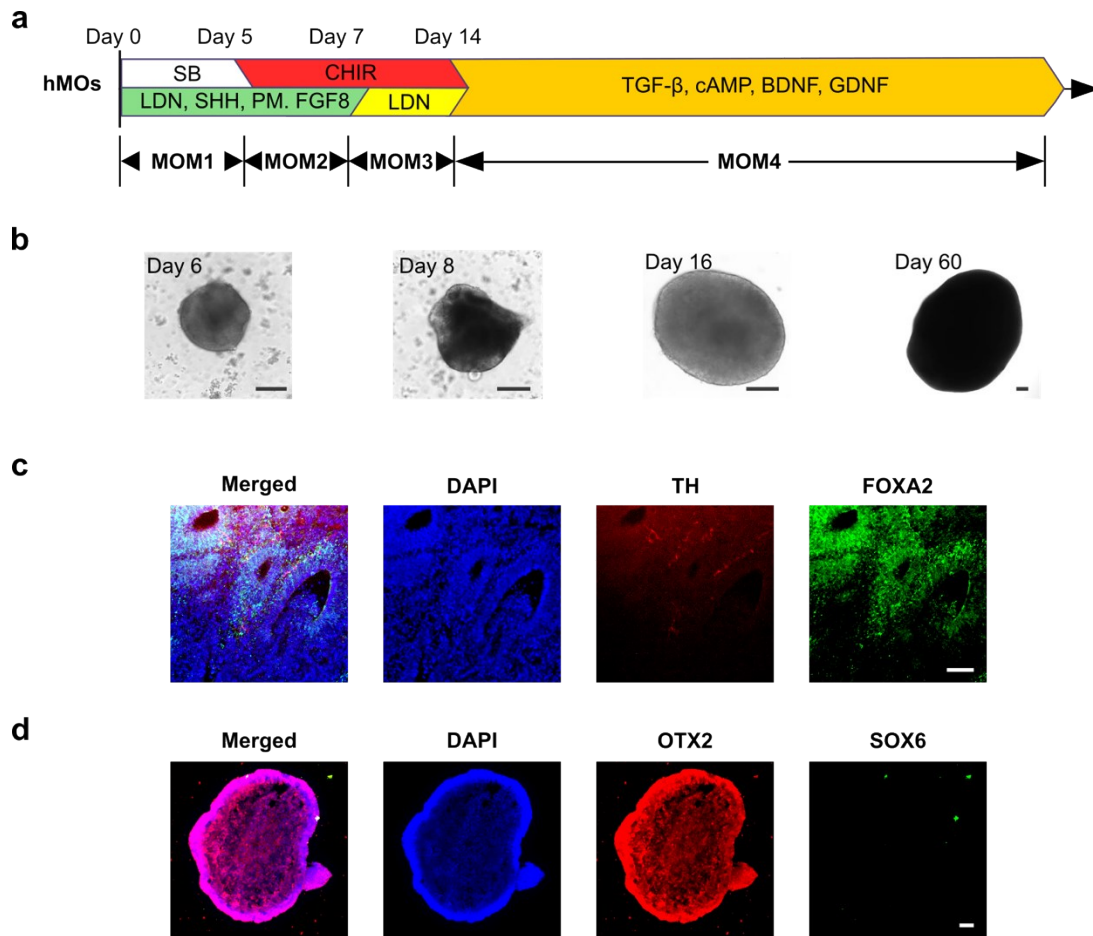


Figure S2. Fabrication and characterization of human midbrain organoids (hMOs). (a) Schematics showing human midbrain organoid fabrication protocol. (b) Human midbrain organoid maturation. Scale bar: 200 μ m (c) Immunofluorescence staining showing human midbrain organoid formation with FOXA2+ floor plate progenitor cells and TH+ dopaminergic neurons. (d) Immunofluorescence showing hMO expressing VTA progenitor marker OTX2 over SN progenitor marker SOX6. Scale bar: 100 μ m.

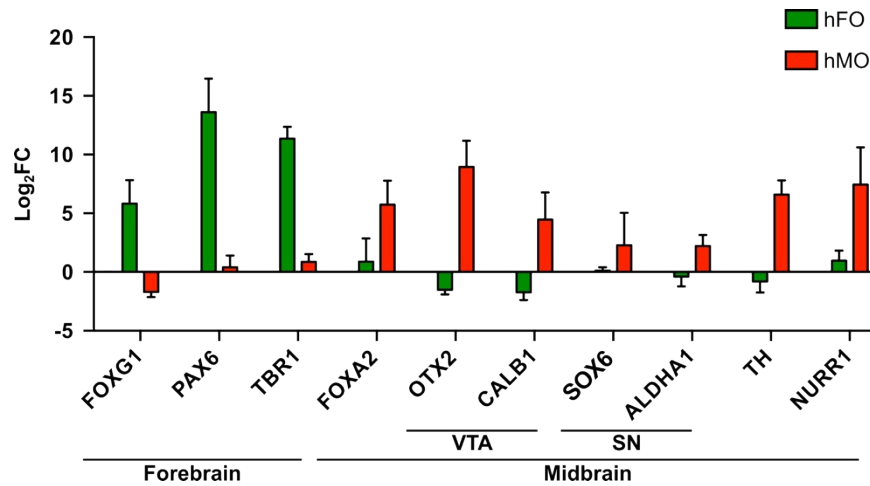


Figure S3. Gene expression analysis of hFOs and hMOs. qPCR analysis of relative gene expression fold changes (FC) of day 35 hFO and hMO over day 1 embryonic bodies (EB) normalized against housekeeping gene GAPDH expression. hFO showed specific expression of forebrain marker expression of FOXG1, PAX6 and TBR1, and hMO showed expression of midbrain markers FOXA2 (floor plate progenitors), high expression of OTX2/CALB1 (VTA region progenitor and mDA neuron makers), moderate expression of SOX6/ALDHA1 (SN region progenitor and mDA neuron markers), and TH/NURR1 (differentiated mDA neuron markers). (n=3)

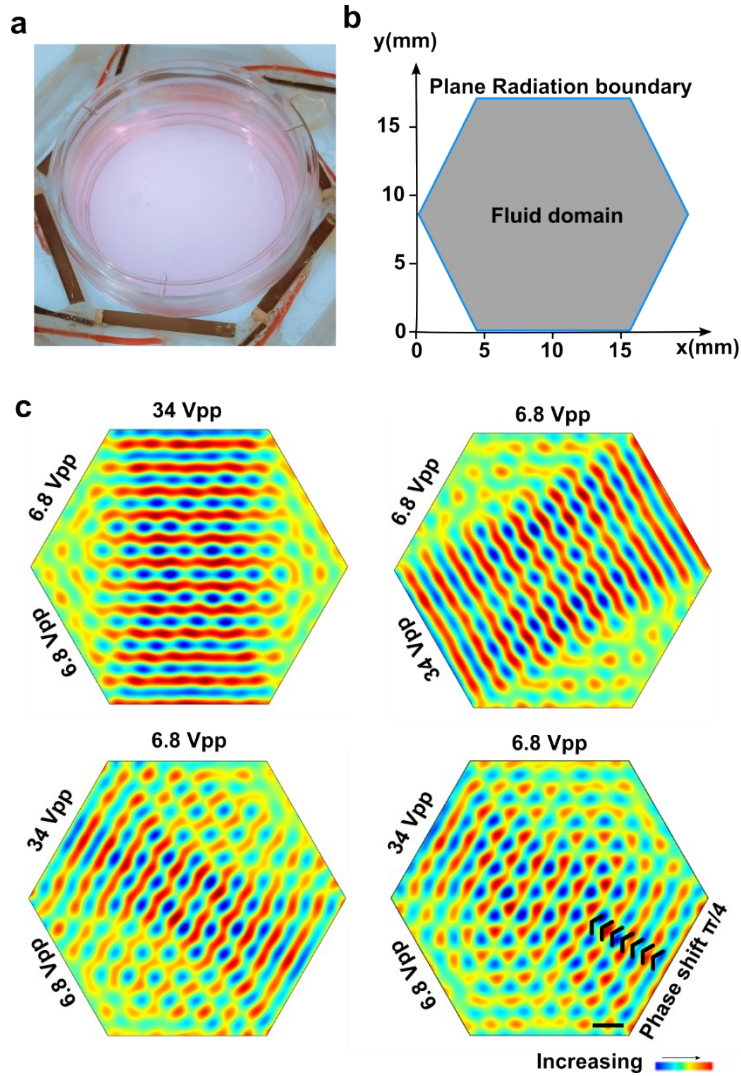


Figure S4. Device image and numerical simulation (a) A photo of the acoustofluidic manipulation device. (b) Simulation model consisting of a hexagon fluidic domain and surrounding plane wave radiation boundary accounting for acoustic waves generated by PZT transducers. (c) A large view of simulation results for acoustofluidic rotational and 2D manipulation. Corresponding to **Figure 2a**. Scale bar: 2 mm

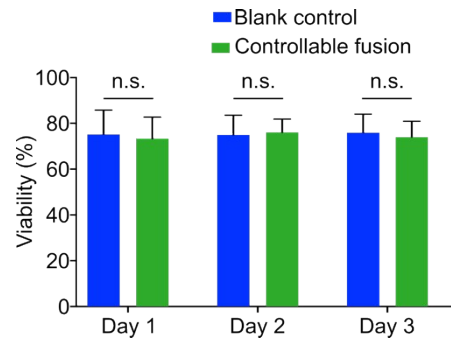


Figure S5. Viability test of organoids after the controllable fusion. To characterize the impact of controllable fusion on assembloid viability, we stained the hFO-hMO assembloids fused via controllable fusion (with acoustic assembly and UV exposure) or random fusion (blank control without acoustic assembly and UV exposure) using a live/dead viability dye from Day 1 to Day 3. We calculated assembloid viability as live cell area (green CFSE stained area)/live cell area+dead cell area (ethidium homodimer stained area). Assembloid maintained high viability except for the dead cells in the hypoxic core area. There is no significant difference between day 1 and day 3 assembloids (viability $75.2 \pm 10.6\%$ versus $76.0 \pm 8.0\%$). We also set up a blank control using U-bottom well based assembly as blank control. We confirmed that there is no significant difference in viability between the two groups.

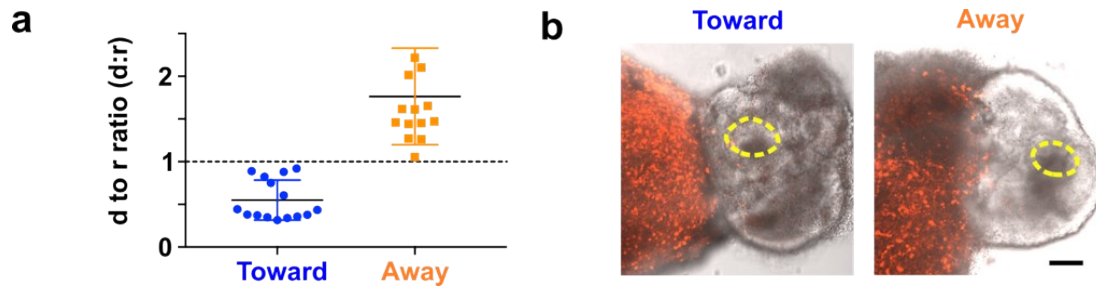


Figure S6. Definition of toward and away assembloids. (a) Comparison of hFO bud distance from hMO in the toward and away group. ($n=15$, $p<0.001$). (b) Representative images of assembloids in the toward and away group. Buds are marked with yellow dotted circles. Scale bar: 100 μm .

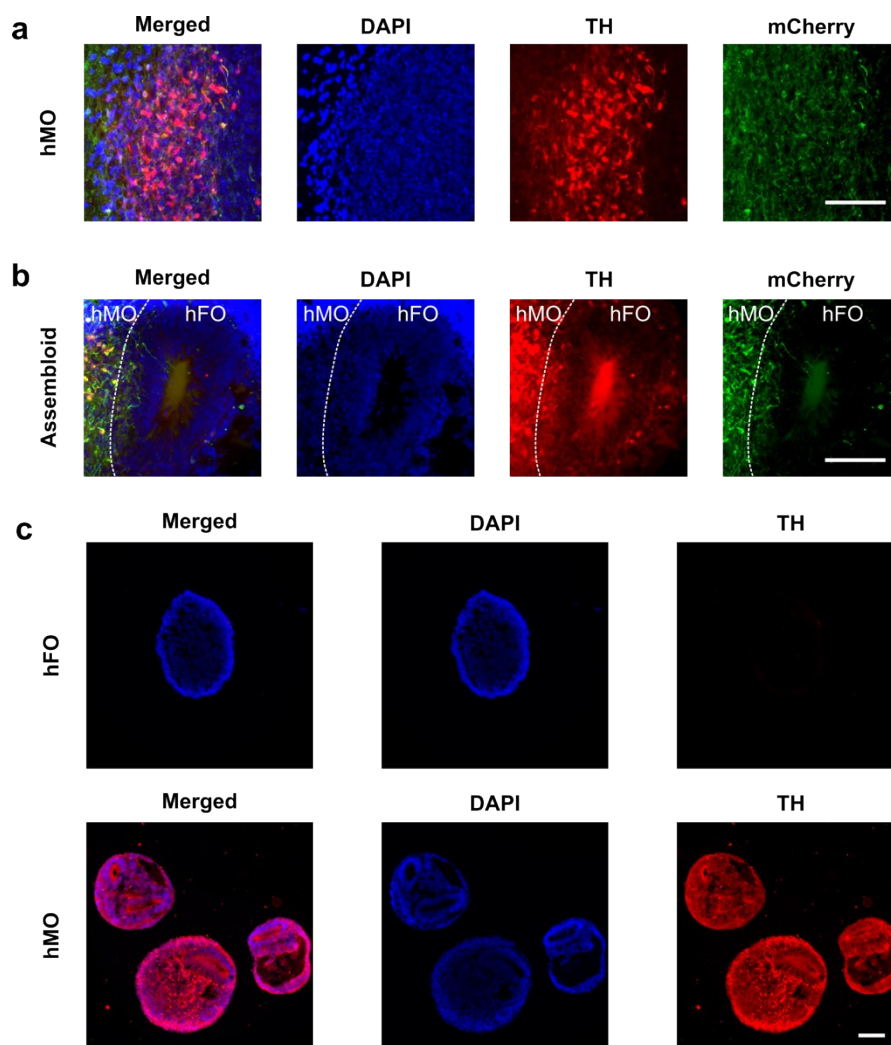


Figure S7. Confirmation of TH neuron origin in the assembloid. (a) TH and mCherry double staining of hMO showing high labeling efficiency of TH neurons in hMO. (b) TH and mCherry double staining of assembloid showing projection hMO neurons are also TH positive. (c) Staining of TH on hMO and hFO alone showed no TH+ neurons in hFO. Scale bar: 100 μ m.

Supplementary Tables

Table S1 Reagents and resources

REAGENT or RESOURCE	SOURCE	IDENTIFIER
Rabbit polyclonal anti-PAX6	Biologend	Cat# 901302; RRID: AB_2749901
Chicken polyclonal anti-MAP2	EMD Millipore	Cat# AB5542; RRID: AB_571049
Goat polyclonal anti-FOXA2	R&D systems	Cat# AF2400; RRID: AB_2294104
Rabbit polyclonal anti-TH	EMD Millipore	Cat# AB152; RRID: AB_390204
Goat polyclonal anti-OTX2	R&D systems	Cat# AF1979; RRID: AB_2157172
Rabbit polyclonal anti-SOX6	Sigma-Aldrich	Cat# HPA001923, RRID:AB_1080065
Chicken polyclonal anti-mCherry	Abcam	Cat# ab205402, RRID:AB_2722769
Chemicals, Peptides, and Recombinant Proteins		
GlutaMax	Invitrogen	Cat# 35050061
MEM-NEAA	Sigma-Aldrich	Cat# M7145
β -mercaptoethanol	Sigma-Aldrich	Cat# M6250
Dorsomorphin	Stemcell Technologies	Cat# 72102
A-83-01	Stemcell Technologies	Cat# 72022
Y-27632	SelleckChem	Cat# S1049
N2 supplement	Invitrogen	Cat# 17502048
CHIR-99021	Stemcell Technologies	Cat# 72052
SB431542	Stemcell Technologies	Cat# 72232
Insulin	Sigma-Aldrich	Cat# I9278-5ML
B27 supplement	Invitrogen	Cat# 17504044
Ascorbic Acid	Sigma-Aldrich	Cat# 1043003
cAMP	Sigma-Aldrich	Cat# A9501
BDNF	Peprtech	Cat# 450-02
GDNF	Peprtech	Cat# 450-10
KOSR	Invitrogen	Cat# 10828028

LDN-193189	Stemcell Technologies	Cat# 72147
SHH	Peprotech	Cat# 100-45
Purmorphamine	Stemcell Technologies	Cat# 72202
FGF8	Peprotech	Cat# 100-25A
ReLeSR	Stemcell Technologies	Cat# 05872
Gelatin methacryloyl (Gel-MA)	Sigma-Aldrich	Cat# 900496-1G
2-Hydroxy-4'-(2-hydroxyethoxy)-2-methylpropiophenone (Irgacure 2959)	Sigma-Aldrich	Cat# 410896-10G
Critical Commercial Assays		
Click-iT EdU Alexa 647 cell proliferation kit	Thermo Scientific	Fisher Cat# C10340
Experimental Models: Cell Lines		
WA01	WiCell	hPSCReg ID: WAe001-A
Recombinant DNA		
pAAV-hSyn-mCherry	Addgene	Cat# 114472; RR_ID: Addgene_114472
pAAV.CamKII.GCaMP6s.WPRE.SV40	Addgene	Cat# 107790; RR_ID: Addgene_107790
pAAV.Syn.GCaMP6s.WPRE.SV40	Addgene	Cat# 100843; RR_ID: Addgene_100843
Software and Algorithms		
ImageJ	NIH	https://imagej.nih.gov/ij/
GraphPad Prism 7	GraphPad	RR_ID: SCR_000306
CalMan	(Giovannucci et al., 2019)	https://github.com/flatironinstitute/CalMan
PySpike	(Mulansky and Kreuz, 2016)	https://github.com/mariomulansky/PySpike
COMSOL Multiphysics 5.2a	COMSOL	https://www.comsol.com/product-download/5.2a/windows
Primers		

Gene	Forward primer	Reverse primer
FOXG1	CGTTCAGCTACAACGCGCTCAT	CAGATTGTGGCGGATGGAGTTC
PAX6	AGTTCTTCGCAACCTGGCTA	ATTCTCTCCCCCTCCTTCCT
TBR1	GACTCAGTTCATCGCCGTCA	TCGTGTCATAATTATCCCGAAATCC
FOXA2	GGGGTAGTGCATCACCTGTT	CCGTTCTCCATCAACAACCT
OTX2	CCAGACATCTTCATGCGAGAG	GGCAGGTCTCACTTTGTTTTG
CALB1	TGTGGATCAGTATGGGCAAAGA	CTCAGTTTCTATGAAGCCACTGT
SOX6	AGGGAGTCTTGCCGATGTG	CAGGCTCTCAGGTGTACCTTTA
ALDHA1	CCGTGGCGTACTATGGATGC	GCAGCAGACGATCTCTTTTCGAT
TH	TGTCTGAGGAGCCTGAGATTCG	GCTTGTCCTTGCGTCACTG
NURR1	GCTGGACTCCCCATTGCTTT	CGGAGCTGTATTCTCCCGAA
GAPDH	GACAGTCAGCCGCATCTTCT	AAATGAGCCCCAGCCTTCTC

Table S2 Medium composition for human forebrain organoid fabrication

Ingredients	Concentrations
Forebrain Medium I (FOM1)	
DMEM/F12	1X
KOSR	20%
GlutaMax	1X
MEM-NEAA	1X
β -mercaptoethanol	1X
Dorsomorphin	2 μ M
A-83-01	2 μ M
Y-27632	5 μ M
Penn/Strep	1X
Forebrain Medium II (FOM2)	
DMEM/F12	1X

N2 supplement	1X
GlutaMAX	1X
MEM-NEAA	1X
CHIR-99021	1 μ M
SB431542	1 μ M
Penn/Strep	1X
Forebrain Medium III (FOM3)	
DMEM/F12	1X
N2 supplement	1X
GlutaMAX	1X
MEM-NEAA	1X
B27	1X
β -mercaptoethanol	1X
Penn/Strep	1X
Insulin	2.5 μ g/mL
Forebrain Medium IV (FOM4)	
Neuralbasal medium	1X
GlutaMAX	1X
MEM-NEAA	1X
B27	1X
Penn/Strep	1X
Ascorbic Acid	0.2 mM
cAMP	0.5 mM
BDNF	20 ng/mL
GDNF	20 ng/mL

Table S3 Medium composition for human midbrain organoid fabrication

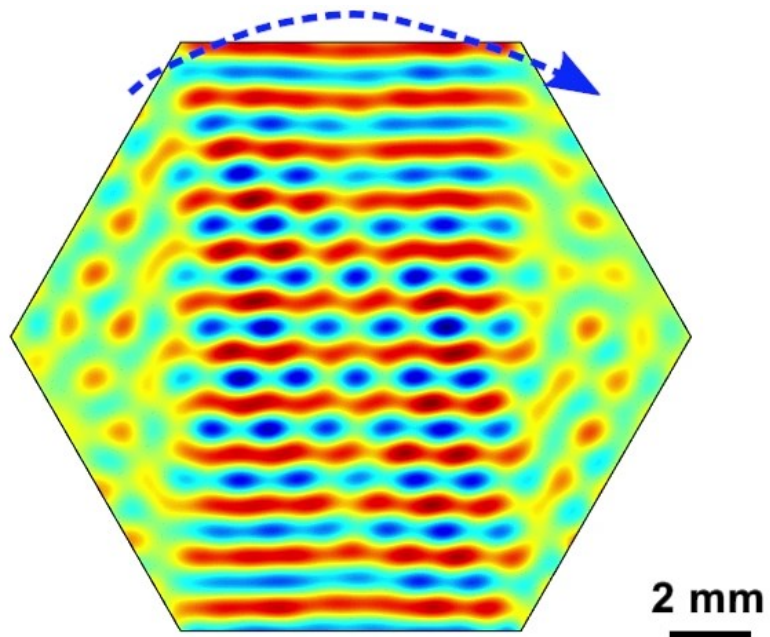
Ingredients	Concentrations
Midbrain Medium I (MOM1)	
DMEM/F12	1X
KOSR	20%
GlutaMax	1X
MEM-NEAA	1X
β -mercaptoethanol	1X
LDN-193189	100 nM
SB-431542	10 μ M
SHH	100 ng/mL
Purmorphamine	2 μ M
FGF8	100 ng/mL
Penn/Strep	1X
Midbrain Medium II (MOM2)	
DMEM/F12	1X
N2 supplement	1X
GlutaMAX	1X
LDN-193189	100 nM
CHIR-99021	3 μ M
SHH	100 ng/mL
Purmorphamine	2 μ M
FGF8	100 ng/mL
Penn/Strep	1X
Midbrain Medium III (MOM3)	
DMEM/F12	1X

N2 supplement	1X
GlutaMAX	1X
MEM-NEAA	1X
LDN-193189	100 nM
CHIR-99021	3 μ M
Penn/Strep	1X
Midbrain Medium IV (MOM4)	
Neuralbasal medium	1X
GlutaMAX	1X
MEM-NEAA	1X
B27	1X
Penn/Strep	1X
Ascorbic Acid	0.2 mM
cAMP	0.5 mM
BDNF	20 ng/mL
GDNF	20 ng/mL

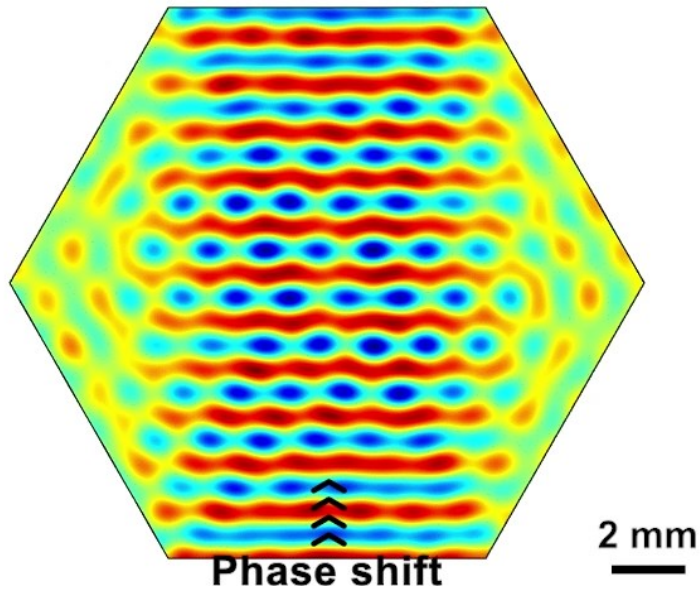
Table S4 Comparison of current spheroid/organoid assembly methods

Criteria	U-bottom plates/tubes	Microfluidic Droplets	Magnetics	Acoustofluidics
Control of spheroid/organoids direction	No	No	No	Yes
Require modification of medium	No	No	Yes	No
Fusion of 3 or more spheroid/organoids	Yes	No	Yes	No

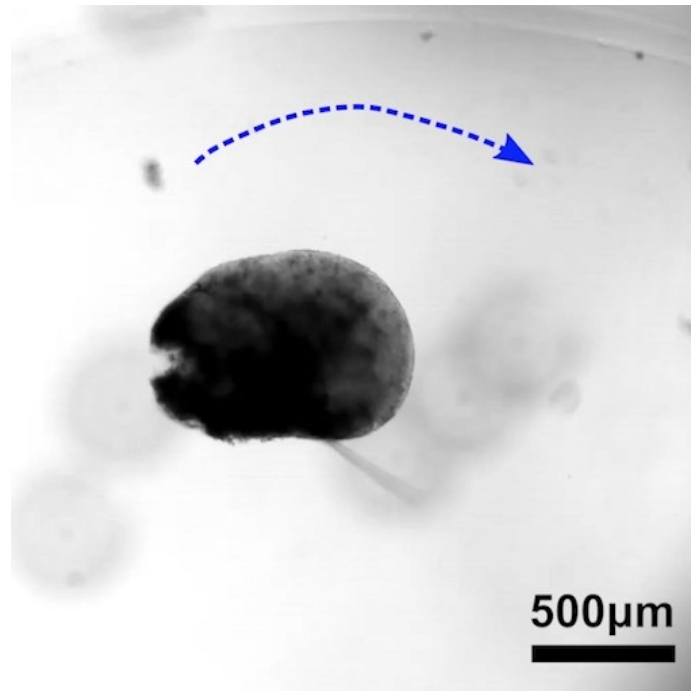
Supplementary Movies



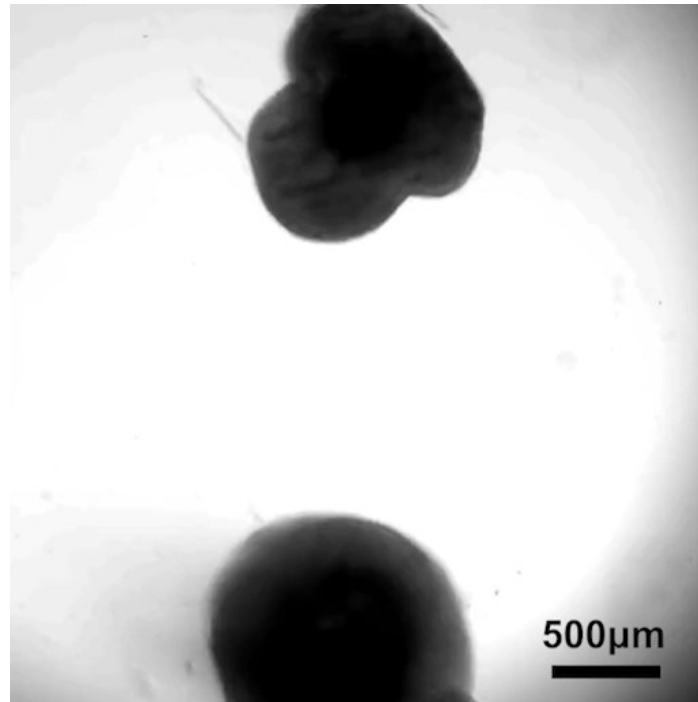
Movie S1. Simulation of rotational manipulation. This movie corresponds to **Figure 2a**. Here, the acoustic field was rotated clockwise for 120° by adjusting the amplitude ratio of PZTs.



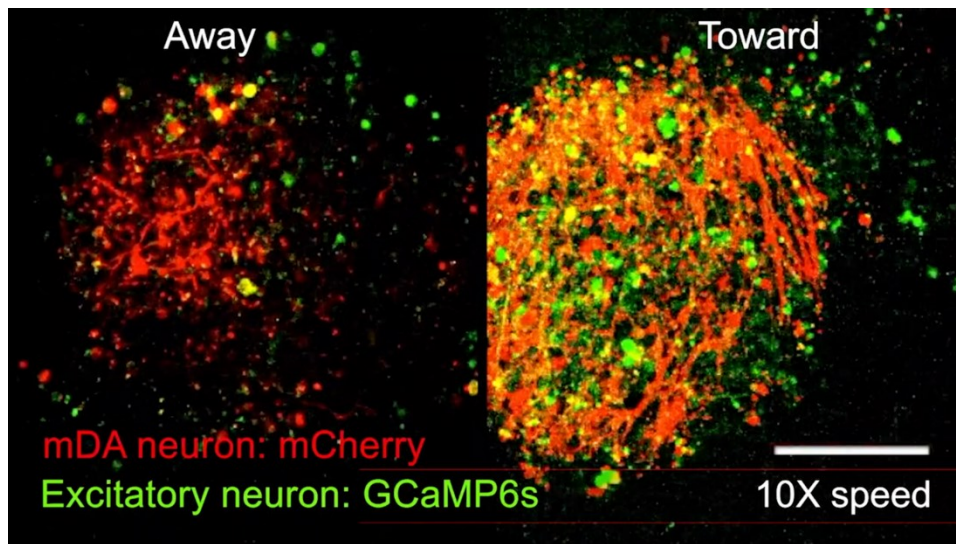
Movie S2. Simulation of transportation via phase shift. This movie corresponds to **Figure 2a**. Here, the phase of the lower PZT in pair 1 is shifted from 0 to 90°.



Movie S3. Acoustofluidic rotation of an hFO. This movie corresponds to **Figure 2b**. Here, the hFO is rotated by gradually switching the amplitudes of three pairs of PZTs among the three combinations. The organoid was trapped along 30, 90, 120, 180, 240, and 300 degrees (to the vertical direction) respectively. The movie is at 4x speed.



Movie S4. The directional fusion of an hFO and an hMO. This movie corresponds to **Figure 2e**. Here, the hFO is rotated and transported to the affixed hMO with a minimized distance of neuroepithelial buds within the hFO to the hMO. The movie is in real-time.



Movie S5. Spontaneous firing of hMO-hFO assembloids. This movie corresponds to **Figure 4c**. Here, projecting TH neurons from the hMO were labeled with mCherry fluorescent protein (red), and spontaneous firing of excitatory neurons was recorded at 10Hz sampling rate from GCaMP6s calcium reporter, the video is sped up 10 times. Scale bar: 200 μ m.